

11-1992

Galactic Structure from Faint Stromgren Photometry: The Catalog of Observations

Ted A. von Hippel
The University Of Michigan

Follow this and additional works at: <https://commons.erau.edu/publication>



Part of the [Stars, Interstellar Medium and the Galaxy Commons](#)

Scholarly Commons Citation

von Hippel, T. A. (1992). Galactic Structure from Faint Stromgren Photometry: The Catalog of Observations. *The Astronomical Journal*, 104(5). <https://doi.org/10.1086/116357>

This Article is brought to you for free and open access by Scholarly Commons. It has been accepted for inclusion in Publications by an authorized administrator of Scholarly Commons. For more information, please contact commons@erau.edu.

11-1992

Galactic Structure from Faint Stromgren Photometry: The Catalog of Observations

Ted A. von Hippel

Follow this and additional works at: <https://commons.erau.edu/publication>



Part of the [Stars, Interstellar Medium and the Galaxy Commons](#)

This Article is brought to you for free and open access by Scholarly Commons. It has been accepted for inclusion in Publications by an authorized administrator of Scholarly Commons. For more information, please contact commons@erau.edu.

GALACTIC STRUCTURE FROM FAINT STRÖMGREN PHOTOMETRY: THE CATALOG OF OBSERVATIONS

TED A. VON HIPPEL

Department of Astronomy, University of Michigan, Ann Arbor, Michigan 48109, and Institute of Astronomy, Madingley Road, University of Cambridge, Cambridge, CB3 0HA, United Kingdom

Received 8 May 1992; accepted 20 July 1992

ABSTRACT

We have initiated a faint photometric survey in the Strömgren system covering ≈ 1 square degree and including 1238 objects in order to develop samples which best probe the thick disk population. The catalog of observations are presented here. They were acquired without kinematic or metallicity biases and are complete to $V=17.3$ – 18.5 , depending on the field, for 810 early to relatively late type (K0 V or G5 III) stars. Photometric metallicities were derived for 508 stars and indicate a metal-poor stellar population, consistent with a mixture of thick disk and halo stars. While the Strömgren u -band was not part of the survey, follow-up u -band observations of 32 survey objects indicate that intermediate color survey stars ($0.3 \leq b-y < 0.5$) are main-sequence or slightly evolved stars, while redder survey stars ($b-y \geq 0.5$) are giants. The survey catalog is available in electronic form upon request.

1. INTRODUCTION

Though the thick disk was first identified in the Galaxy nearly a decade ago (Gilmore & Reid 1983) and has been the subject of much subsequent work (e.g., Norris *et al.* 1985; Wyse & Gilmore 1986, 1988; Norris 1986; Freeman 1987; Sandage 1987; Sandage & Fouts 1987; Norris & Green 1989; Carney *et al.* 1989), its nature is still poorly understood. For instance, some (e.g., Bahcall & Soneira 1980, 1984; Bahcall 1986; Norris 1987; Norris & Ryan 1989; Norris & Green 1989) have argued that the Galaxy is best described as two stellar populations, and that the putative thick disk is the overlap of the extreme tails of the two standard populations rather than a discrete component with its own formation history. To better clarify the nature of the thick disk we have developed a kinematically unbiased stellar selection criteria that strongly favors thick disk stars relative to the contaminating influences of the thin disk and halo components of the Galaxy. The data are presented here and the results are presented in a companion paper (von Hippel & Bothun 1992, hereafter Paper II).

Additionally, in recent years a number of studies (Winget *et al.* 1987; Liebert *et al.* 1988) have exploited the cooling behavior of white dwarf (WD) stars as a function of time in order to date the Galaxy. These studies have yielded an age for the galactic disk of 9.3 ± 2.0 (Winget *et al.* 1987) and 7–10 (Liebert *et al.* 1988) billion years, though the number of WDs in the faintest luminosity bin, with the most power in the age determination, currently stands at only six stars (Hintzen *et al.* 1989). The technique employed to select and study thick disk stars also has the potential of finding cool WDs, and though our survey did not sample enough volume to find any cool WDs, we point out here how the technique could find such objects.

The specific means of selecting thick disk stars (discussed at greater length in Paper II) and of searching for cool white dwarfs was to conduct a faint photometric survey in the Strömgren (Strömgren 1963) system. The

Strömgren filters were selected for their higher quality temperature, metallicity, and surface gravity information than the Johnson broad-band system, though at a cost of being ≈ 5 times slower than the latter system. The Strömgren photometric system employs four intermediate bandpass filters: u , v , b , and y , which are used in conjunction to make three color indices: $b-y$, m_1 , and c_1 ; the temperature, metallicity, and surface gravity sensitive indices, respectively. Since large areal coverage is required in a study such as this, observations using a focal reducing camera (Aldering & Bothun 1991) were made in v , b , and y . The transmitting nature of the camera optics precludes observations at u and therefore those observations could only be done in direct CCD mode which necessarily had quite limited sky coverage. Thus, the observational program consisted of two phases, vby survey observations followed by u -band targeted observations.

Though the surface gravity sensitive filter, the u band, was not employed in the survey, the Strömgren v , b , and y filters also have the ability to photometrically separate WDs. White dwarfs with hydrogen atmospheres (type dA, for nomenclature see McCook & Sion 1987) have strong H δ lines in the v passband and white dwarfs with nonhydrogen atmospheres (usually type dB) have less line opacity in this region than most other stars. This photometric separation between white dwarfs and other stars can be seen in Fig. 1, which presents the standard stars of Perry *et al.* (1987, hereafter POC), along with WD photometry by Graham (1972), and theoretical sequences for cool dA and non-dA WDs by Bergeron (1989). Figure 1 also includes a fourth-order line fit to the POC data, which will be used for comparison with survey data. The POC stars range from supergiants to main-sequence stars, but cover a narrow range in metallicity at nearly the solar value. The models are those described in Bergeron *et al.* (1990) convolved with the Strömgren filters. Temperature in thousands of Kelvins is labeled along the theoretical sequences. This figure demonstrates that white dwarfs, except for

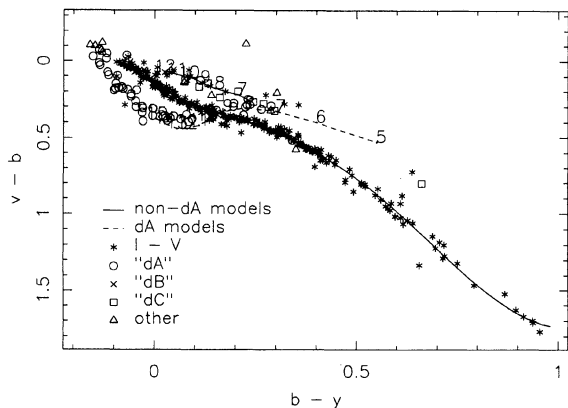


FIG. 1. $v-b$ vs $b-y$ for the POC standard stars, Graham's (1972) white dwarfs and Bergeron's (1989) cool dA and non-dA white dwarf models. Temperature in thousands of Kelvins is labeled for the theoretical sequences. A fourth-order line fit to the POC data is also presented.

those dAs with $T \approx 10\,000$ K, separate photometrically from most other stars. The models and Graham's observations also imply that lower temperature WDs would also separate photometrically from normal stars.

Subdwarf stars separate photometric from solar metallicity stars in the vby plane, as can be seen in Fig. 2, where the line fit for the POC standards is replotted, along with isometallicity lines derived from an inversion of the photometric metallicity calibration of Schuster & Nissen (1989, hereafter SNII). Figure 2 also includes the reddening vector with a length given by a $b-y$ reddening of 0.5 mag. Isometallicity values are given in $[\text{Fe}/\text{H}]$ in the range $-2.0 < [\text{Fe}/\text{H}] < +1.0$ for "F-stars" and $-3.0 < [\text{Fe}/\text{H}] < 0.0$ for "G-stars." In the "F-star" color range, $0.22 < b-y < 0.38$, the derived metallicities are independent of surface gravity. For the "G-star" range, $0.39 < b-y < 0.59$, derived metallicity depends on surface gravity, through the c_1 index. The dashed lines in Fig. 2 represent

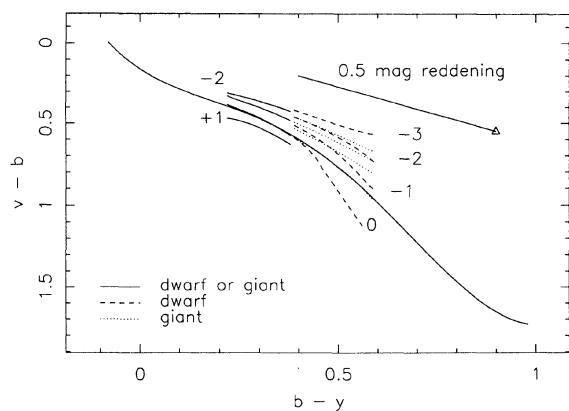


FIG. 2. Isometallicity contours (SN II) in the vby plane, along with the reddening vector and the POC line fit. Isometallicity values are given for $-2.0 < [\text{Fe}/\text{H}] < +1.0$ for F stars and $-3.0 < [\text{Fe}/\text{H}] < 0.0$ for G-stars.

TABLE 1. Field characteristics.

field	RA+Dec	$l(\text{II})$	$b(\text{II})$	v^a	b^a	y^a	v_{limit}	$y_{1.3}$	$y_{1.6}$	$y_{1.9}$	$y_{2.8}$	$E(B-V)$
6	0232+035	165.98	-50.28	9000	5200	4800	18.9	17.6	17.3	17.0	16.1	0.03
7	0410+117	181.10	-27.50	10800	7200	5400	18.8	17.3	17.2	16.9	16.0	0.4
8	0955+247	206.68	51.04	32400	16800	9000	19.4	18.1	17.8	17.5	16.6	0.02
1	1134+300	199.28	73.46	21600	10800	3600	19.8	18.3	18.2	17.9	17.0	0.000
2	1302+283	52.30	86.88	23400	8400	4800	19.8	18.5	18.2	17.9	17.0	0.007
7	0410+117	181.10	-27.50	7200	1200	1200	18.6	17.3	17.0	16.7	15.8	0.4
9	0856+331	191.36	40.04	43200	7200	3900	19.1	17.8	17.5	17.2	16.3	0.015
10	1559+369	58.84	49.00	21600	3600	3600	19.6	18.3	18.0	17.7	16.8	0.005
3	1626+368	59.09	43.59	21600	5400	3000	19.3	18.0	17.7	17.4	16.5	0.005
13	0352+096	179.66	-32.25	30600	4500	3200	18.9	17.6	17.3	17.0	16.1	0.12
14	0913+442	176.75	44.10	33000	3600	3600	18.8	17.5	17.2	16.9	16.0	0.00
4	2129+000	54.26	-34.92	15600	5400	3600	19.2	17.8	17.5	17.3	16.4	0.05
5	0046+051	121.85	-57.44	24300	10800	7200	18.8	17.5	17.2	16.9	16.0	0.03

^a exposure time in seconds

the metallicity calibration for G-dwarfs and the dotted lines represent the metallicity calibration for G-giants.

While the major aim of this paper is to present the survey database, we also derive photometric metallicities for the survey objects (Sec. 3.4) in order to demonstrate the utility of this type of photometry. The interpretation of the metallicity information is not attempted, however, and readers are referred to Paper II where we isolate samples of thick disk and halo stars in order to determine the scale-height and age of the thick disk.

2. OBSERVATIONS AND REDUCTIONS

2.1 Field Selection

Fields were chosen at relatively high galactic latitudes, generally above $b=30^\circ$, to maximize the likelihood and ease of finding low metallicity field stars and cool white dwarfs. Fields were selected covering a wide range of galactic locations to allow observations at nearly any time of year. Care was also taken to avoid significant contamination by known background galaxy clusters and by bright stars ($V \leq 12$) which would saturate sections of the CCD detector.

2.2 Data Acquisition

2.2.1 The survey

The photometry was acquired over eight observing runs between February, 1989 and November, 1990. These observing runs included 60 nights, of which 9 nights from 4 runs were useful. Three photometric or nearly photometric nights were lost to instrument problems, the remaining 48 were lost to poor weather. The coordinates of the observed fields, along with their cumulative exposures, limiting magnitudes, and reddening values are listed in Table 1. The long cumulative exposures were built up from exposures of 600–1800 s (v -band), 400–1200 s (b -band), and 200–300 s (y -band). The derivation and meaning of the limiting magnitudes are discussed below in Sec. 3.3. All survey photometry was collected at the Michigan–Dartmouth–M.I.T. (MDM) Observatory's 1.3 m $f/7.5$ Cassegrain telescope with the OREAD focal-reducing camera (Aldering & Bothun 1991), Strömgren vby filters and a Thomson-CSF TH7861 four-phase blue-enhanced CCD. The focal reducing camera increased the plate scale at the focal point by a factor of 4.67, yielding approximately $1/12$ of a square degree per frame, with a pixel scale of $2.27'' \text{ pixel}^{-1}$. This large gain in field size was essential to the survey, but the

resulting undersampled point spread functions (psf) caused a number of unique instrument and data reduction problems, and some loss in performance.

Though the Strömgren filters used are not identical to those which define the system (Strömgren 1963), they are reducible to the standard system. In particular the b filter was somewhat too wide, the v filter somewhat too narrow, and the transmission of the focal-reducing camera dropped rapidly through the v filter. Effective differences and problems are discussed in Sec. 2.3.1.

Standard stars were observed during three periods each night, during evening and morning twilight and in the middle of the night. Since the POC standards available in the northern hemisphere are all bright ($V \leq 7$), they were observed with the telescope defocused enough to spread their light over ≈ 100 pixels and with very short (1.0 s) exposures. Typical exposures contained many more than 10^4 photons, and errors due to counting statistics alone were usually ≤ 0.004 , 0.002, and 0.002 mag for v , b , and y , respectively. Of greater concern was the reliability of MDM's Uniblitz shutter which was tested by taking various length exposures of bright and faint stars. These tests indicated that this shutter gave precise exposures to better than 0.1%. To remove any remaining shutter precision problems all standards were exposed in all filters for 1.0 s. Thus residual accuracy problems would manifest themselves only as errors in the photometric zero points, the effect on which should be $\leq 1\%$.

2.2.2 u -band

Since the Strömgren u filter is the luminosity class indicator for the Strömgren system, a small, targeted (though randomly selected), u -band follow-up to the general survey was initiated to provide a rough statistical breakdown of the ratio of dwarfs to giants as a function of $b-y$ color. These u -band data were acquired during one photometric night in February, 1991 at the MDM Observatory's 1.3 m $f/7.5$ Cassegrain telescope with the Thomson CCD in direct mode. This combination of telescope and detector gave an image scale of $0.49'' \text{ pixel}^{-1}$. Since the effective seeing on the CCD was $\geq 1.7''$ the images were well-sampled. Objects were chosen from three survey fields available at low airmass (0352+096, 0856+331, and 1302+283), and selected such that as many stars as possible with $11.5 \leq u \leq 20$ would fit on a given CCD frame. Generally three or four stars could be observed simultaneously, yielding measurements for a total of 32 stars. Cumulative exposures ranged from 600 to 3600 seconds to yield photon-counting statistics better than 5% for most stars. Program objects were observed only in the Strömgren u filter since all objects had previously measured v , b , and y magnitudes from the survey. The combined $uvby$ data presented below suffer no additional selection effects beyond those of the general survey, since the u -band observations were randomly targeted follow-up observations of the original survey objects.

Though the Strömgren u filter used is not identical to the one which defines the system (Strömgren 1963), it is reducible to the standard system. Effective differences and

problems are discussed in Sec. 2.3.2. Standard stars were observed in the same manner as for the $uvby$ survey; they were observed during evening and morning twilight and in the middle of the night, with the telescope defocused and with very short (1.0 s) exposures.

2.3 Data Reduction

2.3.1 The survey

All survey photometric data were reduced in a relatively standard manner, except for the techniques involved in "coadding" the data. The data were first bias subtracted using a median bias frame made from a large number of individual biases frames. Since the Thomson dark current is negligible no dark count corrections were made. Flattening was somewhat more difficult due to the strong large-scale structure present in the vignetted field, and possibly due to scattered light. Experimentation showed that twilight sky and dome flats did not have good large-scale characteristics, so median object flats were used instead. Since all fields were predominantly sky anyway, with few stars and no large objects, these flats had excellent ($\approx 0.1\%$) large-scale characteristics. Due to the low sky count rate the pixel-to-pixel random photon counting errors were somewhat higher, however, generally between 0.4% and 1.0%, though occasionally as high as 1.6%, depending on the filter and run. After flattening, the standards were reduced with the IRAF routine SPHOT, which integrates starlight in a specified aperture and subtracts sky as measured in a large annulus about the star. The resulting instrumental magnitudes were analyzed using an algorithm due to Harris *et al.* (1981), which simultaneously solved all photometric transformation coefficients for the standard first order equations:

$$\begin{aligned} y_{\text{true}} &= y_{\text{instr}} + ZP_y + k_y X + c_y (b_{\text{true}} - y_{\text{true}}), \\ b_{\text{true}} &= b_{\text{instr}} + ZP_b + k_b X + c_{b_1} (b_{\text{true}} - y_{\text{true}}), \\ b_{\text{true}} &= b_{\text{instr}} + ZP_b + k_b X + c_{b_2} (v_{\text{true}} - b_{\text{true}}), \\ v_{\text{true}} &= v_{\text{instr}} + ZP_v + k_v X + c_v (v_{\text{true}} - b_{\text{true}}), \end{aligned} \quad (1)$$

where ZP_x is the photometric zero point of the telescope plus detector system for filter x , k_x is the extinction term for filter x , X the airmass, and c_x is the color term for filter x . Since the detector and reducing camera were the same from run to run, the color terms were stable throughout the survey, except where different filters were used. The extinction terms were constrained to the KPNO mean values (0.33, 0.21, 0.16 mag per airmass, from the IRAF extinction files), though the unconstrained extinction terms differed only slightly from these values. The photometric zero points differed from run to run, ranging by ≈ 0.2 mag, due to sky transparency effects and the general cleanliness of the primary mirror. Additionally, the #8 v -band color term was poorly constrained due to poor v -band color coverage among the standards, so was set equal to that found for other runs. The v -band photometry for fields 13, 14, 4, and 5 may thus have higher systematics than those of the other fields, though the color distribution

TABLE 2. Photometric transformations (*vby*).

filter	c_x	ZP_5	s_5	ZP_6	s_6	ZP_7	s_7	ZP_8	s_8
v	-0.15	16.90	0.033	16.80	0.054	16.95	0.033	17.17	0.034
b ₁	0.08	17.86	0.017	17.80	0.023	17.95	0.027	18.01	0.027
b ₂	0.12	17.86	0.014	17.80	0.021	17.95	0.026	18.01	0.025
y	0.11	18.58	0.011	18.52	0.022	18.63	0.026	18.70	0.019

of these fields looked consistent with the fields from the other runs. The final transformation coefficients and their standard deviations for the four useful observing runs, #5–8, are given in Table 2. The conservative uncertainties in the photometric coefficients are: 2%–3% in *v*, 1%–2% in *b*, and 1% in *y* for the airmass terms and $\approx 2\%$ in each filter for the color terms and zero points. There is an additional uncertainty which may be as large as 2% caused by the bootstrapping process, discussed more fully below. The sources of these photometric uncertainties are three-fold: filters which do not precisely match the defining filter system, hydrogen absorption lines falling in the *v* filter, and to a lesser extent the *b* filter, and the short exposure times required for the standards.

Photometry of all objects in the survey fields was performed with standard IRAF tasks. Objects were first identified on each frame as peaks of intensity 3σ or more above the background with the IRAF task *daofind*, then multi-aperture photometry was performed on them with the IRAF task *PHOT*. The reducing camera plus telescope configuration produces a FWHM spot size of 2.0–2.4" over the central $\frac{2}{3}$ of the field (Aldering & Bothun 1991). Thus 1.5–2.0" seeing was expected to produce $\approx 3.6''$ images, requiring an aperture radius of 6.5" (3 pixels) to collect 99% of the light from a point source. Careful experimentation showed that 3-pixel apertures ($n_{\text{pix}}=29$) contained 97% of the light for bright stars (averaged over the entire field), but less than 80% of the light for the faintest stars. This extra degradation in the photometric results was caused primarily by the difficulties *DAOFIND* had in locating the ill-defined centers of faint and undersampled objects, and secondarily by the noncircular psf's near the corners of the field. Since the instrumental counts for most stars were far greater in the *b* and *y* bandpasses than in the *v* bandpass, these brightness-dependent centering difficulties introduced color errors in the 3-pixel aperture photometry. Using 4-pixel apertures ($n_{\text{pix}}=50$) reduced the aperture-induced color errors for the faintest objects considerably, though it added noise from the sky and the CCD. While centering algorithms specially designed for undersampled profiles might decrease the number of pixels required for accurate photometry, the noncircular psf's near the field edges would still require large apertures unless only the inner $\frac{2}{3}$ of a field were photometered. The *OREAD* camera, despite these inherent problems, was still used for its ability to image large fields.

Since accurately registering undersampled data is impossible, at least if flux must be conserved, the ASCII magnitude lists were "coadded," object by object. Since the final coadded photometry required a $S/N \geq 20$ (see Paper II), the objects lost by this technique were too faint to be used even if direct CCD coaddition had been possible.

TABLE 3. Photometric transformations (*u*).

filter	k_x	c_x	ZP	s
u	0.61	0.22	19.44	0.050
v	0.33	0.05	17.65	0.032

Common objects between photometry lists were first identified using an algorithm due to Groth (1986), then the means and standard errors (after 3σ clipping) were computed for all measurements of a particular object. This technique had a number of advantages over standard frame-plus-frame coaddition: it allowed each measurement to be extinction corrected by the airmass relevant over a short time period, it directly determined the photometric error for each object, it allowed easy disposal of bad photometry, and it did not hide any potential object variability. In addition this coaddition technique allowed the data to be internally bootstrapped. Since some of the observations were taken under nonphotometric or marginally photometric conditions, bootstrapping allowed these observations to be corrected. The bootstrapping procedure was to measure the mean brightness of up to 40 bright stars on each frame and scale that frame to the mean as measured for the same stars under photometric conditions. Frames which required scaling by more than an arbitrary cutoff of 33% were discarded. Bootstrapping lowered random errors for any given field considerably, but had the potential of introducing small systematic errors which are conservatively estimated at 2%. Additionally, the basic need to bootstrap some of the data yielded limiting magnitudes for a given field that could not be simply determined based on exposure times, photometric zero points, and mean night sky brightnesses.

2.3.2 *u*-band

All *u*-band photometric data were reduced using essentially the same techniques as used with the survey data, though no enhanced "coadding" was necessary. The data were first bias subtracted using a median bias frame made from a large number of individual bias frames. Since *u*-band sky counts were very low, dark current corrections of 1.5 counts per hour were made for exposures over 1200 s. Flattening was achieved by the use of median twilight sky flats. These had excellent pixel-to-pixel characteristics (flat to $\approx 0.05\%$) and good large-scale characteristics (flat to $\approx 0.55\%$). After flattening, the standards were reduced in the same fashion as the *vby* survey standards. The transformation equations

$$v_{\text{true}} = v_{\text{instr}} + ZP_v + k_v X + c_v (u_{\text{true}} - v_{\text{true}}), \quad (2)$$

$$u_{\text{true}} = u_{\text{instr}} + ZP_u + k_u X + c_u (u_{\text{true}} - v_{\text{true}})$$

were solved as described for the survey standards and yielded the transformation coefficients and their standard deviations given in Table 3. Since the data were taken on only one night the *u*-band extinction term was not constrained to the KPNO mean value of 0.63 (from the IRAF extinction files) but rather the measured value of 0.61 was used. The standards yielded conservative uncertainties in

the u -band photometric coefficients of 2% each for the zero point and color term and 1% for the airmass term. The quality of the transformations are better than those for the general survey primarily because all the data were collected on only one high-quality night. As with the general vby survey photometry, the root causes for the photometric uncertainties are threefold: filters which do not precisely match the defining filter system, hydrogen absorption lines falling in the v filter (used for the color term), and the short exposure times required.

Photometry of all program objects was performed with standard IRAF tasks. Apertures were selected to be large enough to contain 99% of the light from the photometered object. The presentation of these data can be found below.

3. PHOTOMETRIC RESULTS

3.1 Survey Photometry

Table 4 presents the reddening corrected photometry catalog of 1238 objects in order of increasing Right Ascension (RA). Field numbers are provided in column 1 before each field, and are listed in the order 5.0, 6.0, 13.0, 7.0, 9.0, 14.0, 8.0, 1.0, 2.0, 10.0, 3.0, 4.0, since fields are ordered by RA. Note that Table 1 also lists the match between field numbers and equatorial coordinates, as well as galactic coordinates. For each data entry in Table 4, column 1 lists the CCD id number, columns 2 and 3 list the Right Ascension and Declination (Dec) (1950), column 4 lists the apparent V magnitude, columns 5 and 6 list $b-y$ and $v-b$ color, columns 7, 9, and 11 list photometric standard errors for the v , b , and y measurements, and columns 8, 10, and 12 list the number of measurements in v , b , and y for each object. No sign is listed before the Dec, as all values are positive. RA and Dec were determined using IRAF finder, which computes positions based on the ST guide stars it finds in the field, and coordinates should be accurate to within ≈ 2 arcsec. Internal precision in the coordinates is probably somewhat better, and is expected to be ≈ 0.6 arcsec. The data presented in Table 4 are available in electronic form upon request.

The “complete” portion of the catalog (defined below), after reddening correction (discussed below), is also plotted in Figs. 3(a)–3(l), along with the galactic coordinates for each field and the POC line fit from Fig. 1. The POC line fit is derived from solar metallicity stars in the solar neighborhood and is meant to provide a ready way to assess the differences between fields. Close agreement is not expected between the POC line fit and the data as the survey contains a large number of objects of less than solar metallicity. All objects plotted in Figs. 3(a)–3(l) are brighter than the limiting magnitude $y_{1.6}$ given for that field as listed in Table 1 and discussed in the next section. The photometric color errors are indicated by the error bars of length one standard error. Many of the photometric outliers are the result of crowded photometry. A few of the reddest outliers are M II or M III stars, which may stray far from the POC line fit. While a detailed discussion of these data is taken up in Paper II, it can be seen here that these faint, high galactic latitude stars are predominantly

of intermediate or red color and, based on their colors relative to the POC line fit, cover a wide range of metallicity with an upper metallicity limit approximately equal to the solar value. A small random subset of these survey objects were followed up in the Strömgren u filter, and are discussed below in Sec. 3.5.

3.2 Reddening

Most of the survey stars are at distances great enough for interstellar reddening to be significant, though no means of determining reddening internal to the survey (e.g., Strömgren $H\beta$ photometry) exists. For this reason the Burstein & Heiles (1982, hereafter BH) reddening maps were used. BH give galactic reddening in $E(B-V)$ [$=1.35 E(b-y)$, BH] along most lines of sight based on integrated H I density and background galaxy counts. While these reddening values are intended for extragalactic objects they should be appropriate for the bulk of the survey stars which, even if dwarfs, lie at distances greater than 500 pc. The BH reddening values yield reddening corrected photometry which appears consistent from field to field except for the field at $b = -28^\circ$. BH give $E(B-V) = 0.24$ for this field but it is near a steep reddening gradient, and their maps have a beam size of nearly 1 square degree. The BH value seemed to be an underestimate and it was found that $E(B-V) = 0.40$ was the most consistent with the colors of stars from other fields. Uncertain reddening for this one field has little effect on the statistics of the survey database, however, since 12 separate fields were observed. Additionally, most reddening corrections are only a few hundredths of a magnitude (see Table 1), so even significant errors in their values will have minimal effect on the derived results. The reddening corrected photometry are presented in Figs. 3(a)–3(l), and discussed in detail below.

3.3 Estimating Completeness

After transforming all photometry to the standard system, the standard deviation of the observations themselves were used to determine the survey depth. Most survey objects were observed repeatedly and therefore have measured photometric standard deviations. Even objects which were only detected once in each filter have theoretical standard deviations since photon counting statistics are assumed to have a Poisson distribution. The distribution of photometric standard deviations as a function of apparent y magnitude for a representative field is plotted in Fig. 4, along with lines corresponding to 4σ and 5σ detections. It can be seen in this figure that the photometric standard deviations increase with apparent magnitude, and that the error in the v -band are at least as great as those in the b -band, and far greater than those in the y -band. This is a consequence of the much higher throughput of the telescope, reducing camera, and detector combination in the redder passbands, and of the fact that most stars have significantly more flux in the red. Thus, the photometric errors in the v -band represent the majority of the random error in the observations, and it is safe to characterize the

TABLE 4. Strömgren survey photometry.

id	RA	Dec	V	b-y	v-b	e_v	n_v	e_b	n_b	e_y	n_y	id	RA	Dec	V	b-y	v-b	e_v	n_v	e_b	n_b	e_y	n_y
5.0												68	2 32 44.1	3 25 28	18.18	0.33	0.69	0.339	1	0.172	1	0.004	7
8	0 45 52.1	5 09 54	14.73	0.70	1.06	0.003	3	0.001	13	0.001	14	71	2 32 49.9	3 28 48	11.86	0.68	1.00	0.001	6	0.000	18	0.001	4
2	0 45 53.3	5 09 13	13.40	0.69	0.86	0.003	6	0.001	17	0.000	16	76	2 32 50.8	3 21 07	15.32	0.50	0.68	0.005	3	0.001	17	0.000	23
6	0 45 54.4	5 07 44	16.46	0.50	0.68	0.024	1	0.001	10	0.001	27	75	2 32 51.7	3 29 50	15.14	0.36	0.47	0.003	4	0.001	17	0.000	24
18	0 45 56.7	5 04 42	17.08	0.34	0.52	0.043	1	0.002	8	0.001	26	79	2 32 51.9	3 25 43	13.72	0.44	0.57	0.001	4	0.000	17	0.000	24
23	0 45 57.3	5 03 21	17.69	0.33	0.50	0.007	2	0.006	4	0.002	19	80	2 32 53.8	3 22 32	17.44	0.39	0.45	0.024	2	0.004	4	0.002	19
43	0 45 59.5	4 59 52	18.79	0.83	-4.49	0.003	15	0.013	3	0.010	4	81	2 32 54.2	3 23 31	16.81	0.39	0.54	0.076	1	0.002	12	0.001	24
51	0 46 01.6	5 08 12	16.69	0.39	0.68	0.027	1	0.001	9	0.001	27	83	2 32 55.4	3 22 52	16.67	0.44	0.60	0.002	2	0.001	9	0.002	24
70	0 46 04.8	5 13 13	14.15	0.43	0.67	0.003	6	0.001	15	0.000	23	82	2 32 55.5	3 33 22	17.51	0.34	0.47	0.006	2	0.001	3	0.002	17
74	0 46 05.2	5 02 15	18.82	0.50	0.22	0.153	1	0.005	3	0.003	3	84	2 32 56.3	3 30 25	16.89	1.03	1.21	0.036	3	0.002	6	0.001	22
75	0 46 05.4	5 11 27	18.57	0.48	0.23	0.138	1	0.013	3	0.007	6	983	2 32 57.0	3 34 20	14.80	0.59	0.85	0.004	4	0.001	13	0.000	24
76	0 46 05.5	5 07 45	14.94	0.39	0.56	0.003	6	0.001	18	0.000	29	87	2 32 58.5	3 32 58	17.58	0.49	0.72	0.031	3	0.009	2	0.003	20
83	0 46 06.8	5 09 37	14.23	0.34	0.48	0.002	9	0.000	19	0.000	29	69	2 32 58.5	3 21 20	18.47	0.44	1.20	0.074	2	0.005	2	0.008	6
98	0 46 09.1	5 07 40	15.05	0.49	0.73	0.004	6	0.000	17	0.000	29	70	2 33 01.0	3 21 15	17.54	0.41	0.70	0.020	3	0.003	3	0.002	17
97	0 46 09.1	5 08 27	17.65	0.83	0.80	0.061	1	0.026	1	0.002	19	94	2 33 01.0	3 20 32	13.63	0.39	0.57	0.002	6	0.001	12	0.000	23
109	0 46 10.8	5 11 20	17.72	0.63	1.02	0.066	1	0.010	3	0.002	17	95	2 33 02.2	3 28 47	13.91	0.37	0.47	0.001	6	0.001	17	0.000	24
111	0 46 10.9	5 09 32	17.86	0.47	0.81	0.010	3	0.003	4	0.002	15	90	2 33 02.9	3 29 28	13.09	0.59	0.84	0.002	4	0.000	18	0.000	24
112	0 46 11.2	5 12 03	13.55	0.42	0.62	0.001	10	0.001	20	0.000	29	92	2 33 03.2	3 26 26	17.08	0.46	0.59	0.100	1	0.005	4	0.002	23
115	0 46 11.3	5 05 05	15.80	0.53	0.80	0.017	2	0.001	18	0.001	28	260	2 33 03.4	3 32 15	17.36	-0.35	2.65	0.307	1	0.062	1	0.188	1
118	0 46 12.1	5 12 18	14.70	0.53	0.78	0.003	8	0.001	20	0.001	29	95	2 33 08.0	3 21 59	16.26	0.53	0.80	0.004	2	0.002	12	0.001	24
120	0 46 12.2	4 59 51	18.89	0.69	-1.38	0.174	2	0.232	1	0.008	4	102	2 33 08.5	3 22 35	15.10	0.46	0.62	0.006	5	0.000	16	0.000	24
128	0 46 13.9	4 59 38	17.41	0.39	-0.24	0.001	2	0.003	5	0.003	16	103	2 33 09.5	3 28 10	14.87	0.46	0.60	0.004	5	0.001	17	0.000	24
132	0 46 14.7	5 10 39	18.01	0.55	0.66	0.024	3	0.008	2	0.003	13	85	2 33 11.3	3 21 42	17.33	0.45	0.74	0.113	1	0.004	5	0.002	18
145	0 46 16.4	5 04 34	17.05	0.48	0.71	0.007	3	0.001	6	0.001	24	118	2 33 13.3	3 23 30	14.74	0.43	0.59	0.001	2	0.001	17	0.000	24
147	0 46 16.8	5 12 45	19.20	0.58	-0.22	0.281	1	0.246	1	0.177	1	122	2 33 15.8	3 30 26	16.32	0.47	0.56	0.004	2	0.001	14	0.033	1
164	0 46 20.1	5 13 37	15.63	0.38	0.49	0.005	4	0.001	16	0.001	29	132	2 33 17.0	3 22 43	12.87	0.44	0.61	0.003	7	0.000	18	0.000	24
173	0 46 21.5	5 08 45	14.02	0.44	0.64	0.002	8	0.001	19	0.000	29	133	2 33 17.3	3 27 31	12.74	0.38	0.48	0.001	5	0.000	17	0.000	24
177	0 46 22.0	5 10 59	15.71	0.42	0.59	0.005	5	0.001	17	0.001	29	132	2 33 17.5	3 26 00	10.94	0.33	0.41	0.005	2	0.001	5	0.002	2
182	0 46 23.0	5 00 47	19.23	1.08	-0.22	0.372	1	0.006	2	0.000	2	96	2 33 18.7	3 24 13	17.01	0.41	0.54	0.053	3	0.003	8	0.002	23
180	0 46 28.2	5 02 43	19.72	-0.51	-0.29	0.349	1	0.194	1	0.482	1	141	2 33 19.3	3 22 58	14.33	0.46	0.62	0.002	5	0.000	17	0.001	24
146	0 46 28.7	5 13 29	18.01	0.60	0.69	0.301	2	0.009	3	0.006	11	149	2 33 21.6	3 28 10	12.00	0.44	0.62	0.002	6	0.000	18	0.000	3
204	0 46 28.8	5 01 40	15.21	0.39	0.48	0.003	3	0.001	18	0.000	29	341	2 33 21.8	3 25 22	18.22	0.39	-0.11	0.086	1	0.015	3	0.000	6
206	0 46 29.0	5 12 11	18.68	0.75	-0.19	0.180	1	0.067	1	0.006	5	103	2 33 23.6	3 24 50	13.60	0.56	0.96	0.006	1	0.001	9	0.000	23
212	0 46 29.5	5 01 33	14.38	0.31	0.72	0.002	6	0.001	20	0.001	29	403	2 33 24.8	3 31 19	17.87	0.39	0.32	0.105	1	0.009	3	0.003	12
213	0 46 29.9	5 05 20	13.95	0.33	0.43	0.001	10	0.000	20	0.000	29	107	2 33 26.3	3 23 18	16.08	0.76	1.28	0.015	2	0.002	14	0.001	23
222	0 46 31.5	5 01 15	12.78	0.37	0.69	0.001	12	0.000	20	0.003	24	110	2 33 27.0	3 26 12	16.06	0.45	0.65	0.044	1	0.001	11	0.058	1
199	0 46 31.9	4 59 12	16.42	0.50	0.74	0.022	3	0.005	4	0.002	6	112	2 33 27.8	3 29 11	16.67	0.46	0.59	0.009	3	0.002	9	0.002	23
226	0 46 32.7	5 03 18	17.40	0.91	1.06	0.116	3	0.008	2	0.002	23	108	2 33 28.0	3 33 54	16.04	0.77	0.85	0.002	3	0.004	9	0.001	23
251	0 46 36.7	5 03 18	18.30	0.86	0.60	0.101	1	0.040	3	0.015	7	117	2 33 28.3	3 27 02	16.74	0.61	0.99	0.073	1	0.002	4	0.004	15
255	0 46 37.5	5 06 11	15.61	0.54	0.75	0.009	3	0.001	16	0.000	29	918	2 33 29.4	3 28 54	16.35	0.53	0.57	0.037	1	0.002	12	0.001	23
259	0 46 38.0	5 03 50	15.32	0.62	0.88	0.005	4	0.001	18	0.000	29	120	2 33 31.4	3 31 44	16.65	0.91	1.12	0.003	2	0.007	8	0.002	20
267	0 46 39.6	5 02 22	17.89	0.81	1.11	0.067	2	0.003	3	0.003	14												
270	0 46 39.9	5 03 31	16.59	0.59	0.86	0.018	2	0.002	10	0.001	29	13.0											
271	0 46 40.5	5 05 24	16.21	0.43	0.55	0.018	2	0.001	16	0.001	27	3	3 51 31.5	9 43 24	17.09	0.36	0.53	0.024	3	0.056	2	0.027	3
279	0 46 42.2	5 12 43	17.53	0.85	0.78	0.041	3	0.006	3	0.002	24	4	3 51 33.1	9 32 42	15.54	0.36	0.53	0.003	6	0.007	9	0.003	15
295	0 46 43.8	5 02 46	16.37	0.43	0.53	0.004	3	0.001	16	0.001	28	6	3 51 33.6	9 44 15	15.55	0.37	0.49	0.002	4	0.003	12	0.001	16
293	0 46 43.9	5 09 48	15.93	0.48	0.62	0.015	3	0.001	14	0.001	29	9	3 51 33.9	9 40 06	13.09	0.68	0.92	0.001	19	0.001	13	0.000	19
303	0 46 45.3	5 04 14	18.77	0.35	-0.64	0.167	1	0.080	1	0.007	3	13	3 51 34.0	9 35 51	18.22	0.43	0.78	0.136	1	0.063	1	0.010	9
308	0 46 46.3	5 03 13	17.92	0.58	0.87	0.184	1	0.049	2	0.002	14	24	3 51 36.3	9 44 24	14.15	0.36	0.49	0.001	16	0.001	17	0.000	19
313	0 46 47.2	5 02 55	14.44	0.45	0.57	0.002	5	0.000	19	0.000	29	28	3 51 36.9	9 31 28	17.01	0.58	0.83	0.070	3	0.002	6	0.002	17
344	0 46 54.0	5 12 04	16.42	0.60	0.90	0.023	1	0.001	11	0.001	29	26	3 51 37.1	9 41 07	19.03	-0.51	0.64	0.448	1	0.282	3	0.008	3
346	0 46 54.2	5 11 51	17.28	0.34	0.65	0.009	1	0.053	1	0.003	11	29	3 51 37.2	9 42 30	17.75	0.89	0.30	0.098	1	0.003	3	0.004	14
350	0 46 54.4	5 07 48	17.22	0.56	1.05	0.061	1	0.017	6	0.013	19	32	3 51 37.7	9 42 32	18.03	0.50	0.42	0.074	2	0.061	2	0.014	8
360	0 46 55.5	5 09 18	19.04	0.64	0.11	0.191	1	0.002	3	0.003	2	35	3 51 38.0	9 33 58	18.24	0.33	0.4						

TABLE 4. (continued)

Table with columns: id, RA, Dec, V, b-y, v-b, e_v, r_v, e_s, n_s, e_y, n_y. It contains two columns of data, one starting at id 277 and another starting at id 341, with a gap between them. The table lists astronomical data for various stars, including magnitudes and color indices.

TABLE 4. (continued)

Table with columns: id, RA, Dec, V, b-y, v-b, e_v, n_v, e_b, n_b, e_y, n_y, id, RA, Dec, V, b-y, v-b, e_v, n_v, e_b, n_b, e_y, n_y. The table contains two columns of data, with the second column starting at id=575. It lists various astronomical objects with their coordinates and photometric measurements.

TABLE 4. (continued)

Table with columns: id, RA, Dec, V, b-y, v-b, e_v, n_v, e_b, n_b, e_y, n_y. It lists astronomical data for two sets of objects, with the second set starting at id 81. The table contains two columns of data, each with 100 rows of entries.

TABLE 4. (continued)

id	RA	Dec	V	b-y	v-b	ϵ_r	n_r	ϵ_b	n_b	ϵ_y	n_y	id	RA	Dec	V	b-y	v-b	ϵ_r	n_r	ϵ_b	n_b	ϵ_y	n_y
381	16 00 27.9	36 54 58	18.55	0.36	0.31	0.053	3	0.036	3	0.012	3	239	16 26 54.4	36 53 33	17.81	0.38	0.31	0.047	1	0.000	4	0.021	4
3.0												240	16 26 55.4	37 01 19	14.30	0.75	1.14	0.003	3	0.001	6	0.001	6
3	16 25 46.5	36 59 06	16.72	0.54	0.43	0.024	1	0.005	4	0.053	3	246	16 26 56.6	36 50 59	16.01	0.43	0.56	0.005	3	0.002	5	0.003	6
4	16 25 46.8	37 01 36	13.98	0.50	0.70	0.040	7	0.003	4	0.004	3	251	16 26 57.9	36 49 57	17.38	0.43	0.55	0.069	2	0.009	6	0.011	6
9	16 25 47.7	36 59 20	16.50	0.41	0.43	0.010	2	0.017	4	0.015	3	250	16 26 58.3	37 02 47	19.15	0.79	0.50	0.031	2	0.015	3	0.019	1
11	16 25 48.7	37 01 09	18.37	-0.05	0.56	0.145	1	0.201	1	0.149	2	258	16 27 00.4	36 52 56	17.63	0.39	0.45	0.015	3	0.004	3	0.192	5
15	16 25 49.8	36 59 45	17.24	0.48	0.47	0.023	3	0.013	3	0.003	3	261	16 27 01.3	36 51 53	13.06	0.38	0.55	0.014	14	0.001	7	0.003	2
20	16 25 50.8	37 02 50	18.56	0.75	0.87	0.131	1	0.004	3	0.026	4	263	16 27 02.5	37 00 22	17.72	0.78	0.87	0.057	1	0.003	2	0.002	3
22	16 25 51.5	37 00 41	15.85	0.39	0.43	0.003	4	0.003	6	0.002	6	264	16 27 02.7	36 53 57	16.49	0.38	0.51	0.002	3	0.001	4	0.003	5
23	16 25 51.6	36 58 21	18.78	0.70	0.36	0.211	3	0.304	1	0.009	2	266	16 27 03.2	36 57 59	14.46	0.46	0.65	0.002	7	0.001	5	0.001	3
24	16 25 51.8	36 59 06	16.75	0.43	0.44	0.020	1	0.005	5	0.007	6	268	16 27 03.5	36 49 18	14.51	0.12	0.25	0.015	13	0.001	6	0.001	6
26	16 25 52.7	36 54 53	18.02	0.58	0.86	0.001	2	0.029	3	0.014	5	271	16 27 04.1	36 50 35	18.24	0.50	0.66	0.076	1	0.004	2	0.041	3
29	16 25 54.3	36 49 51	13.76	0.56	0.75	0.001	5	0.003	1	0.001	5	274	16 27 04.4	36 57 59	16.60	0.49	1.28	0.038	1	0.004	3	0.152	3
28	16 25 54.4	36 54 55	17.23	0.56	0.61	0.002	2	0.011	3	0.005	3	275	16 27 05.5	36 57 55	16.26	0.64	0.93	0.007	3	0.004	5	0.010	6
31	16 25 55.8	37 00 21	18.16	0.58	0.66	0.000	1	0.122	1	0.017	5	280	16 27 05.7	36 52 40	15.90	-0.01	0.06	0.002	8	0.002	5	0.002	5
36	16 25 57.4	36 50 23	18.50	0.84	0.80	0.233	1	0.031	3	0.036	4	279	16 27 06.9	37 00 20	17.13	0.33	0.43	0.004	1	0.008	4	0.007	4
37	16 25 58.1	36 58 52	17.93	0.68	0.68	0.068	1	0.001	2	0.010	3	282	16 27 06.4	36 51 14	14.45	0.40	0.49	0.001	7	0.001	6	0.001	6
43	16 25 58.5	36 49 13	15.32	0.44	0.55	0.003	4	0.003	5	0.001	6	284	16 27 07.3	36 49 18	13.90	0.40	0.54	0.106	13	0.005	7	0.001	6
42	16 25 58.5	36 50 09	15.36	0.51	0.81	0.003	5	0.001	4	0.002	6	286	16 27 07.9	36 58 13	18.76	0.88	0.72	0.118	1	0.099	3	0.192	1
45	16 25 58.7	36 50 45	17.40	0.45	0.48	0.009	3	0.004	5	0.009	5	289	16 27 09.3	36 57 32	13.24	0.41	0.61	0.017	13	0.003	7	0.005	1
41	16 25 58.7	36 54 00	20.02	-0.02	0.23	0.226	1	0.041	3	0.001	2	294	16 27 09.6	36 49 23	17.50	0.59	0.59	0.015	3	0.052	4	0.046	5
44	16 25 58.8	36 55 40	19.38	0.29	-0.01	0.157	1	0.047	3	0.065	3	295	16 27 10.2	36 57 27	13.57	0.42	0.58	0.015	14	0.009	7	0.002	4
50	16 26 00.7	37 00 23	18.53	0.91	0.51	0.077	3	0.013	2	0.038	3	305	16 27 11.7	36 56 55	18.98	0.42	0.50	0.064	3	0.215	1	0.038	3
53	16 26 01.1	36 49 03	18.07	0.59	0.54	0.004	2	0.020	2	0.014	3	306	16 27 11.7	36 51 09	17.88	0.33	0.33	0.048	1	0.007	4	0.046	1
55	16 26 01.5	36 52 11	14.36	0.40	0.48	0.001	7	0.001	6	0.001	6	312	16 27 12.9	36 54 39	19.39	0.37	0.48	0.190	1	0.331	1	0.037	3
54	16 26 01.6	36 53 40	17.99	0.56	0.86	0.001	2	0.033	1	0.019	6	317	16 27 14.2	36 51 22	18.18	0.38	0.48	0.074	1	0.017	2	0.018	3
56	16 26 01.6	36 51 15	19.66	0.92	0.33	0.348	1	0.071	1	0.016	3	320	16 27 15.1	37 01 38	15.96	0.39	0.44	0.011	1	0.004	6	0.001	3
60	16 26 01.9	36 52 30	17.86	0.21	0.46	0.085	1	0.031	2	0.015	2	323	16 27 15.2	36 53 11	16.28	0.38	0.44	0.008	3	0.002	5	0.007	3
58	16 26 02.4	36 57 33	19.98	0.42	0.67	0.111	2	0.002	2	0.008	3	325	16 27 15.4	36 49 33	15.63	0.53	0.61	0.002	5	0.007	2	0.002	5
64	16 26 03.5	36 54 57	16.06	0.31	0.33	0.006	7	0.004	6	0.004	6	331	16 27 16.6	37 01 47	17.37	0.45	0.57	0.020	2	0.030	2	0.035	5
67	16 26 04.3	36 49 51	15.48	0.42	0.58	0.000	2	0.001	5	0.001	6	332	16 27 16.8	37 01 58	16.81	0.49	0.77	0.023	1	0.002	5	0.011	6
71	16 26 05.1	37 01 24	16.67	0.51	0.65	0.021	1	0.010	5	0.004	4	347	16 27 19.9	36 58 48	18.72	0.49	0.60	0.149	2	0.027	2	0.052	3
74	16 26 05.6	36 58 41	16.89	0.37	0.46	0.007	3	0.011	5	0.006	4	349	16 27 20.5	36 55 15	18.35	1.02	0.83	0.108	2	0.229	3	0.048	2
78	16 26 06.2	36 50 45	16.13	0.41	0.56	0.006	2	0.004	5	0.003	6	474	16 27 22.2	36 54 48	18.21	0.48	0.39	0.067	2	0.006	3	0.021	2
77	16 26 06.4	36 57 51	14.99	0.42	0.49	0.001	5	0.002	6	0.002	6	475	16 27 22.6	36 54 55	18.26	0.41	0.36	0.093	2	0.016	3	0.027	3
80	16 26 06.8	36 59 42	17.50	0.94	1.00	0.227	2	0.031	2	0.006	3	329	16 27 23.1	36 54 23	18.12	0.50	0.69	0.065	1	0.070	1	0.057	2
82	16 26 07.5	36 58 27	19.12	0.44	0.39	0.178	1	0.273	1	0.008	2	364	16 27 24.7	37 00 41	17.71	0.36	0.34	0.053	2	0.003	3	0.039	1
83	16 26 08.2	36 57 37	16.64	0.49	0.62	0.007	2	0.004	5	0.005	6	368	16 27 24.9	36 49 42	17.58	0.54	0.80	0.016	3	0.016	3	0.022	2
84	16 26 08.6	36 56 02	17.92	0.44	0.55	0.003	1	0.002	4	0.010	2	502	16 27 27.9	36 56 32	17.73	0.36	0.79	0.103	1	0.017	3	0.028	2
86	16 26 08.5	36 51 01	16.41	0.39	0.50	0.004	2	0.004	5	0.003	5	508	16 27 28.4	36 48 58	17.71	1.27	0.83	0.106	2	0.161	1	0.016	3
85	16 26 08.6	36 54 29	15.28	0.45	0.60	0.002	4	0.005	7	0.003	6	377	16 27 28.8	36 54 54	18.51	0.51	0.33	0.108	2	0.022	2	0.052	2
90	16 26 09.0	36 48 59	12.78	0.36	0.46	0.014	14	0.002	4	0.004	2	379	16 27 29.0	37 01 24	17.39	0.34	0.52	0.013	2	0.009	5	0.011	6
96	16 26 11.2	36 54 22	16.06	0.39	0.38	0.003	3	0.002	4	0.002	4	380	16 27 29.3	36 58 11	17.96	0.75	0.73	0.070	1	0.026	3	0.011	3
100	16 26 12.8	36 58 47	17.89	0.43	0.47	0.016	2	0.005	2	0.013	3	385	16 27 31.4	37 02 45	18.60	0.32	0.48	0.118	1	0.003	2	0.075	2
105	16 26 13.0	36 49 10	18.50	1.20	0.46	0.175	1	0.084	1	0.038	3	390	16 27 32.3	36 56 15	16.45	0.41	0.66	0.004	3	0.006	4	0.009	4
102	16 26 13.3	37 02 32	17.12	0.37	0.41	0.022	2	0.014	6	0.012	6	397	16 27 33.0	36 55 34	16.14	0.59	0.97	0.013	2	0.004	4	0.003	6
104	16 26 13.3	36 52 56	15.51	0.51	0.62	0.004	3	0.002	5	0.002	6	399	16 27 33.1	36 57 50	17.74	0.51	0.51	0.052	1	0.009	2	0.010	3
107	16 26 14.0	36 50 02	17.83	0.37	0.40	0.044</																	

TABLE 4. (continued)

id	RA	Dec	V	b-y	v-b	ϵ_v	n_v	ϵ_b	n_b	ϵ_y	n_y	id	RA	Dec	V	b-y	v-b	ϵ_v	n_v	ϵ_b	n_b	ϵ_y	n_y
201	21 29 25.9	0 13 06	19.47	-0.49	0.83	0.578	1	0.430	1	0.018	2	513	21 29 58.4	0 05 54	18.27	0.54	0.54	0.056	3	0.010	3	0.007	8
181	21 29 25.9	0 04 05	19.14	0.51	-0.20	0.240	1	0.038	2	0.016	3	518	21 29 59.2	0 08 09	18.12	0.59	0.30	0.012	2	0.009	3	0.007	8
187	21 29 26.7	0 01 44	17.35	0.86	0.83	0.945	1	0.010	5	0.003	15	517	21 29 59.3	0 08 51	18.14	0.76	0.66	0.086	1	0.012	2	0.004	8
191	21 29 27.2	0 01 57	18.10	0.41	0.68	0.171	2	0.020	2	0.004	10	525	21 30 00.0	0 01 22	18.36	0.43	0.53	0.120	1	0.019	9	0.004	6
174	21 29 28.5	0 15 05	16.24	0.53	0.91	0.028	2	0.024	2	0.083	1	527	21 30 00.0	0 02 03	15.78	0.69	0.90	0.004	2	0.003	9	0.008	18
206	21 29 28.5	0 05 55	17.64	0.59	0.54	0.024	3	0.014	5	0.003	11	526	21 30 00.1	0 03 28	15.56	0.44	0.59	0.005	4	0.002	11	0.001	18
210	21 29 28.5	0 02 04	17.82	0.51	0.75	0.020	3	0.001	3	0.006	14	943	21 30 00.2	0 02 10	15.99	0.42	0.76	0.083	1	0.008	2	0.041	1
216	21 29 29.4	0 06 49	17.60	0.39	0.64	0.056	3	0.006	5	0.004	15	529	21 30 00.5	0 12 44	14.32	0.40	0.52	0.002	8	0.002	12	0.000	18
214	21 29 29.5	0 13 21	17.43	0.44	0.59	0.005	2	0.008	6	0.000	15	537	21 30 01.5	0 06 39	15.08	0.38	0.45	0.004	4	0.002	11	0.001	18
226	21 29 30.3	0 01 03	13.97	0.43	0.61	0.002	3	0.001	9	0.000	17	541	21 30 02.4	0 09 54	16.52	0.49	0.61	0.023	1	0.003	10	0.002	17
224	21 29 30.5	0 08 50	17.58	0.54	0.82	0.090	3	0.009	3	0.003	17	543	21 30 02.6	0 12 51	17.54	0.70	0.43	0.022	3	0.007	3	0.007	12
247	21 29 30.9	0 14 55	18.04	0.03	0.34	0.118	3	0.042	1	0.081	3	389	21 30 02.8	0 15 03	17.62	0.52	0.50	0.022	2	0.167	1	0.143	1
228	21 29 30.9	0 11 34	17.57	0.52	1.05	0.059	1	0.016	3	0.004	13	553	21 30 03.7	0 09 29	17.99	0.39	0.74	0.099	1	0.011	4	0.008	11
232	21 29 31.0	0 00 54	15.13	0.44	0.45	0.006	8	0.003	8	0.002	15	557	21 30 04.4	0 12 42	17.47	0.37	0.42	0.050	1	0.006	4	0.004	17
279	21 29 31.6	0 10 08	17.88	0.38	0.63	0.086	1	0.011	9	0.002	8	562	21 30 05.1	0 06 27	17.29	0.38	0.53	0.017	3	0.005	7	0.004	17
244	21 29 31.7	0 00 52	16.64	0.62	0.31	0.034	3	0.009	6	0.009	15	566	21 30 05.4	0 02 31	17.56	0.61	0.67	0.021	3	0.000	2	0.003	14
288	21 29 31.8	0 11 02	13.44	0.38	0.56	0.001	8	0.002	12	0.000	18	567	21 30 05.6	0 02 54	18.52	0.42	0.46	0.020	3	0.017	3	0.008	7
241	21 29 32.0	0 12 00	17.36	0.39	0.61	0.050	1	0.007	5	0.004	15	570	21 30 06.0	0 07 27	18.73	0.42	0.69	0.174	1	0.019	2	0.007	3
246	21 29 32.2	0 11 15	16.03	0.20	0.12	0.013	10	0.002	11	0.004	18	585	21 30 07.3	0 09 46	14.98	0.40	0.41	0.009	13	0.002	9	0.001	18
249	21 29 32.3	0 04 54	17.03	0.47	0.62	0.013	2	0.008	7	0.002	16	584	21 30 07.4	0 14 29	18.32	0.75	0.57	0.104	1	0.009	3	0.007	5
250	21 29 32.7	0 08 38	18.21	0.34	0.47	0.039	2	0.011	3	0.006	8	588	21 30 07.5	0 01 24	11.41	0.36	0.47	0.002	4	0.023	2	0.001	6
257	21 29 33.3	0 12 43	18.20	0.41	0.21	0.146	3	0.011	3	0.003	7	589	21 30 07.7	0 09 33	16.95	0.52	0.36	0.023	2	0.006	7	0.010	18
256	21 29 33.3	0 13 37	13.01	0.52	0.75	0.001	11	0.002	11	0.002	18	594	21 30 07.9	0 06 09	15.72	0.79	1.00	0.089	1	0.045	7	0.013	17
259	21 29 33.5	0 13 05	17.37	0.17	1.36	0.138	1	0.040	6	0.014	13	598	21 30 08.2	0 04 37	16.94	0.58	0.81	0.053	2	0.002	3	0.002	17
262	21 29 33.9	0 10 42	17.78	0.37	0.52	0.022	3	0.003	3	0.002	11	605	21 30 09.3	0 00 46	15.20	0.45	0.51	0.006	3	0.007	8	0.002	11
264	21 29 34.2	0 12 16	17.69	0.59	0.94	0.057	2	0.003	3	0.002	11	606	21 30 09.6	0 05 55	12.27	0.61	0.79	0.001	13	0.002	10	0.001	6
275	21 29 35.4	0 03 51	17.19	0.52	0.65	0.174	1	0.007	5	0.004	18	607	21 30 09.7	0 06 33	18.14	-0.04	1.48	0.172	1	0.275	1	0.070	7
279	21 29 36.1	0 02 28	16.32	0.47	0.61	0.039	1	0.004	9	0.001	18	610	21 30 10.0	0 02 08	16.89	0.46	0.45	0.008	2	0.004	7	0.003	15
282	21 29 36.4	0 17 54	17.83	0.54	-0.12	0.323	1	0.033	3	0.01	9	613	21 30 10.2	0 03 52	19.38	0.60	0.09	0.442	1	0.197	1	0.028	3
286	21 29 36.7	0 06 12	18.48	0.32	0.61	0.188	1	0.01	2	0.007	5	615	21 30 10.5	0 07 05	17.73	0.24	1.13	0.183	1	0.109	2	0.012	11
288	21 29 36.7	0 02 01	18.76	0.23	0.53	0.123	2	0.001	2	0.243	1	619	21 30 10.8	0 06 49	16.19	0.58	0.54	0.018	3	0.007	9	0.005	18
285	21 29 36.9	0 08 56	19.25	0.76	-0.10	0.285	1	0.022	2	0.151	1	617	21 30 10.9	0 14 13	18.01	0.08	0.25	0.003	2	0.149	1	0.007	10
294	21 29 37.2	0 04 11	14.47	0.48	0.60	0.002	5	0.002	12	0.000	18	627	21 30 11.1	0 03 00	18.87	0.73	0.14	0.025	2	0.014	2	0.009	3
292	21 29 37.3	0 10 12	17.10	0.41	0.59	0.042	1	0.006	7	0.004	18	626	21 30 11.3	0 07 27	16.60	0.47	0.59	0.038	3	0.057	2	0.014	5
319	21 29 38.0	0 14 21	14.78	0.42	0.59	0.004	5	0.003	10	0.001	16	631	21 30 11.5	0 00 39	17.54	0.68	0.86	0.058	1	0.007	2	0.016	6
304	21 29 38.5	0 08 00	16.40	0.62	0.80	0.028	2	0.003	8	0.001	17	628	21 30 11.9	0 13 35	17.44	0.39	0.46	0.030	2	0.005	3	0.005	14
306	21 29 38.9	0 09 11	16.93	0.36	0.50	0.035	1	0.003	6	0.001	16	638	21 30 12.3	0 06 44	13.81	0.48	0.58	0.003	13	0.001	10	0.000	18
314	21 29 39.0	0 04 47	17.91	0.86	0.58	0.072	1	0.057	2	0.008	10	633	21 30 12.3	0 12 36	16.87	0.46	0.47	0.040	2	0.007	5	0.003	17
312	21 29 39.1	0 09 49	15.61	0.42	0.59	0.004	5	0.002	11	0.001	18	637	21 30 12.4	0 09 55	15.05	0.71	0.85	0.009	7	0.012	9	0.001	18
315	21 29 39.1	0 02 59	14.45	0.35	0.45	0.002	4	0.002	12	0.000	18	640	21 30 12.6	0 11 25	14.56	0.41	0.51	0.003	12	0.001	11	0.000	18
316	21 29 39.3	0 06 46	13.54	0.37	0.50	0.001	10	0.002	12	0.001	18	644	21 30 13.0	0 10 04	14.43	0.73	1.00	0.005	7	0.006	10	0.001	18
313	21 29 39.3	0 13 11	18.46	0.89	-0.01	0.169	1	0.085	2	0.012	5	652	21 30 13.7	0 03 11	18.79	0.41	0.53	0.171	1	0.020	2	0.004	3
318	21 29 39.6	0 12 40	15.65	0.47	0.68	0.006	5	0.002	12	0.001	18	658	21 30 14.0	0 04 23	17.94	0.57	0.43	0.076	1	0.016	3	0.009	10
320	21 29 39.6	0 04 51	17.33	0.92	-0.01	0.341	3	0.018	3	0.003	17	656	21 30 14.2	0 11 29	16.18	0.45	0.44	0.008	5	0.003	9	0.002	18
330	21 29 40.5	0 03 46	17.02	0.56	0.78	0.034	1	0.008	7	0.003	18	671	21 30 15.9	0 04 07	18.80	0.50	-0.83	0.166	1	0.009	2	0.010	4
333	21 29 40.6	0 03 10	15.03	0.40	0.52	0.007	3	0.002	11	0.001	18	677	21 30 16.1	0 00 56	15.77	0.49	0.39	0.011	3	0.208	4	0.015	12
336	21 29 40.8	0 02 16	17.78	0.70	0.89	0.085	1	0.024	3	0.004	10	680	21 30 16.3	0 02 12	18.35	0.79	0.52	0.126	1	0.036	2	0.019	6
338	21 29 41.3	0 10 59	18.42	0.38	0.30	0.120	1	0.028	2	0.006	5	679	21 30 16.4	0 04 20	18.21	0.37	0.62	0.127	1	0.006	3	0.009	6
349	21 29 42.4	0 07 03	18.03	0.97	0.53	0.065	2	0.092	1	0.004	9	682	21 30 16.9	0 01 05	12.65	0.43	0.41	0.001	11	0.013	8	0.001	4
354	21 29 42.5	0 05 54	17.02	0.51	0.47	0.008	3	0.029	4	0.005	14	681	21 30 17.1	0 12 31	17.67	0.51	0.94	0.068	1	0.011	3	0.006	13
355	21 29 42.9	0 07 43	11.26	0.43	0.63	0.001	8	0.017	2	0.010	6	687	21 30 17.5	0 00 40	15.33	0.33	0.58	0.017	4	0.044	4	0.017	8
358	21 29 43.1	0 13 20	17.52	0.34	0.52	0.000	2	0.009	5	0.004	15	691	21 30 17.5	0 01 00	13.90	0.42	-0.02	0.007	3	0.057	3	0.011	11
367	21 29 44.0	0 01 08	17.73	0.49	0.48	0.063	1	0.009	4														

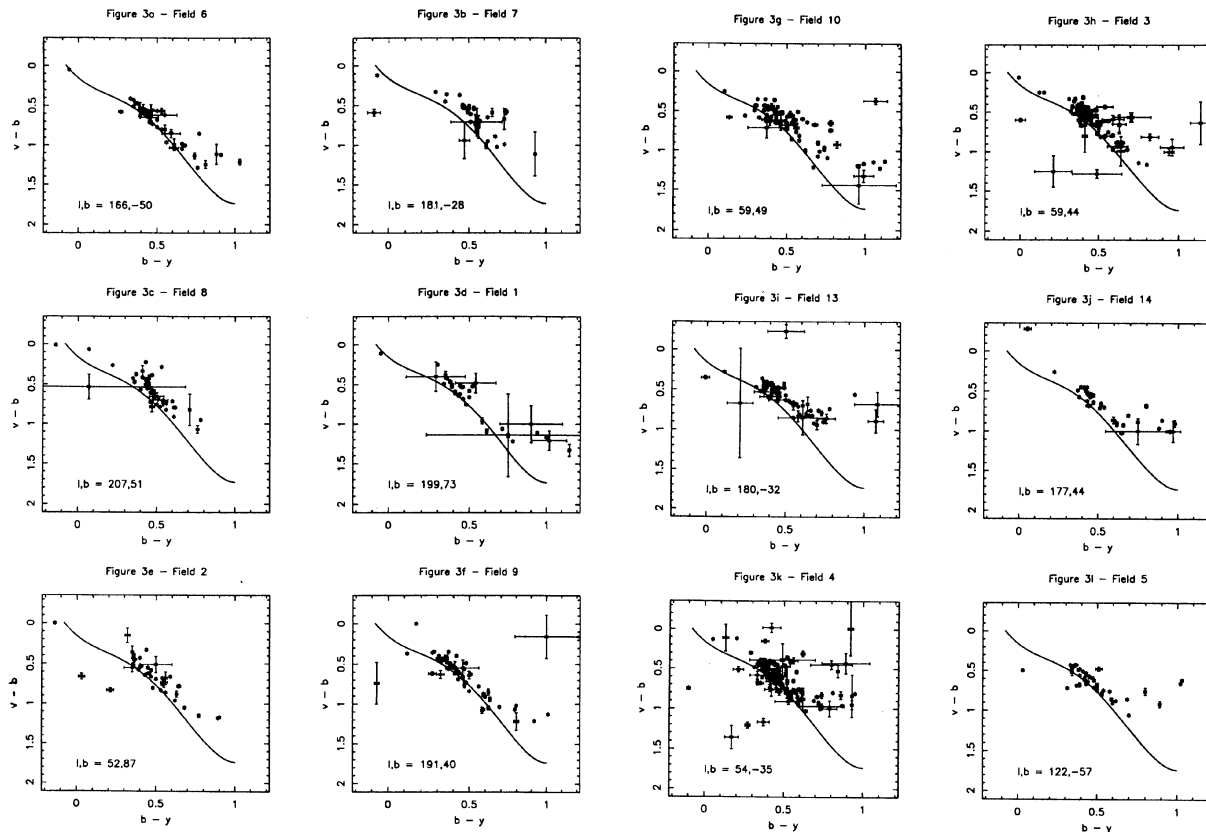


FIG. 3. (a)–(l): $v-b$ vs $b-y$ for the “complete” portion of the reddening corrected catalog, along with the galactic coordinates for each field and the POC line fit. Photometric color errors are indicated by the error bars of length one standard error. Field names are: (a) 6; (b) 7; (c) 8; (d) 1; (e) 2; (f) 9; (g) 10; (h) 3; (i) 13; (j) 14; (k) 4; (l) 5.

depth of the survey as the ability to make detections in the v -band. Analysis of plots like Fig. 4 for each field then allow the computation of conservative limiting magnitudes based upon the v -band photometric standard deviations. Since the minimum criterion for finding an object was that its intensity be 3σ above the background in the v -band,

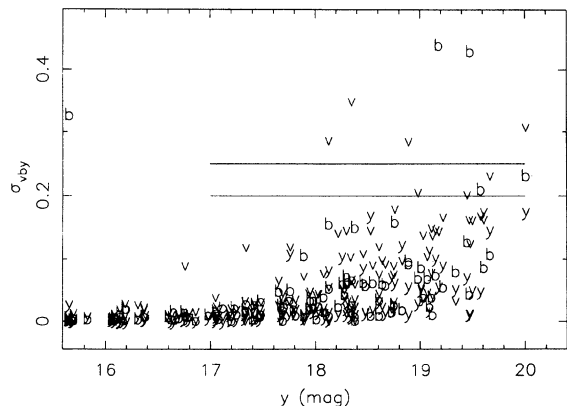


FIG. 4. Distribution of photometric standard deviations as a function of apparent y magnitude for a representative field, along with lines corresponding to 4σ and 5σ detections. The plotting symbols represent the Strömgren bands of the same name.

objects with true v -band brightnesses $\geq 4\sigma$ above the background should have been found in almost all cases. Such objects would have a S/N of ≈ 4 in an individual measurement and an expected standard deviation after many measurements of 25%. Selecting the magnitude where the upper envelope of the v -band standard deviations reaches 20% (an even more conservative 5σ detection) should provide a robust estimate of survey completeness. Incompleteness was estimated for each field using this technique and the results are listed in Table 1. Limiting magnitudes range from 17.3–18.5 in the y -band, or from 18.6–19.8 in the v -band. It should also be noted that Fig. 4 underestimates the photometric quality of the survey database, since most stars were observed 4 to 16 times, and thus their photometric standard errors are generally a factor of 2 to 4 less than their photometric standard deviations. Additionally, since photometric errors are generally considerably less in the y -band than in the other bands, number count analyses based on y -band measurements are even more secure.

The survey first becomes incomplete for two classes of objects; those which happen to fall near the edge of the vignettted CCD, and those which are very red. Stars in the former class are of no real concern when trying to derive populations statistics, since their distribution as a function of stellar type is random, and since they include less than

10% of the stars in any given field. Nonetheless, in estimating incompleteness, the increased photometric errors for these stars have generally been taken into account, and few of these stars brighter than the listed completeness limit should be missing. The latter type of incompleteness, due to color, must be dealt with more carefully. Color is a selection criterion for the faintest objects since detection in the v filter is the most difficult. To quantify completeness as a function of color, Table 1 lists $y_{1.3}$, $y_{1.6}$, $y_{1.9}$, and $y_{2.8}$ magnitudes which correspond to completeness within (i.e., bluer than) four different $v-y$ colors limits. These color limits are at $v-y=1.3, 1.6, 1.9,$ and 2.8 and are equivalent to $b-y=0.5, 0.6, 0.7,$ and 1.0 , or $\approx K0 V$ (G2 III), K4 V (G8 III), K5 V (K1 III), and M1 V (M0 III) stars, respectively (Ardeberg & Lindgren 1985; their calibration is for solar metallicity stars and is used for comparison purposes only, subdwarfs of a given spectral type are bluer). Thus each field becomes incomplete for stars redder than a given color at these listed y completeness magnitudes. Of the 1238 objects in the survey, 810 stars remain within the $y_{1.3}$ complete portion. Results based on these data (e.g., Paper II) should be truncated at the appropriate incompleteness limits for the colors of the stars under study in order to avoid color biases.

3.4 Derivation of Metallicities

Examination of the survey objects in Figs. 3(a)–3(1) indicates that most fields have a lower envelope at or above the POC line fit. This lower envelope is the approximate upper metallicity limit of the stars in each of these fields. Inspection of the isometallicity lines of Fig. 2 quantifies this interpretation. Greater discussion of the derivation of metallicities from these data are taken up in Paper II, where it is shown that average (internal) metallicity random errors are ≈ 0.22 dex and external systematics are probably ≈ 0.3 – 0.4 dex. Additionally, objects with photometric $[\text{Fe}/\text{H}] < -2.6$ are extrapolations.

There are 508 stars with photometric metallicities among the survey stars of which 22% are F-stars. The metallicities of the remaining 78% depend on which luminosity class they are assigned to. If it is assumed that all G-stars are dwarfs then the metallicity distribution represented by a solid line in Fig. 5 results. If the metallicities of the G-stars are assigned on the basis that 10% are giants and 90% are dwarfs, as indicated by the Strömgren u -band follow-up work (discussed further below), then the dashed line of Fig. 5 results. The differences between these two metallicity distributions can be understood by referring to Fig. 2 and noticing that the giant star isometallicity lines are spaced closer together than the dwarf star isometallicity lines.

3.5 u -band

The full set of 32 u by observations are presented in Table 5. The objects are identified in column 1 by the field names from Table 1 and the id from Table 4. Columns 2–5 list the V magnitudes and $b-y$, $v-b$, and $u-v$ colors, respectively. Columns 6–9 list the internal photometric

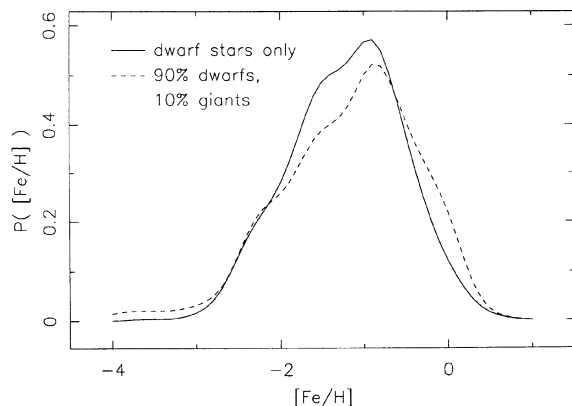


FIG. 5. Generalized histogram of photometric metallicities for the survey stars, of which 22% are F-stars. The solid line represents the assumption that the remainder are all dwarfs, whereas the dashed line represents the assumption that of the remainder 10% are giants and 90% are dwarfs.

standard errors for each color, truncated at two digits after the decimal point. Errors listed as 0.00 are simply less than 0.01 mag, though they are usually ≈ 0.003 mag. Internal errors in the u -band are generally only a few percent, though a few of the fainter objects have standard errors of $\approx 10\%$. Systematic errors of a few percent cannot be ruled out. The data in Table 5 have been corrected for reddening by the same $E(B-V)$ values used for the survey data (from BH, and listed in Table 1).

The u by observations are also presented in Fig. 6, in the form of the c_1 vs $b-y$ diagram, which can be thought of as similar to an HR diagram. The $c_1 [= (u-v) - (v-b)]$ index was designed to measure the surface gravity of F-stars (Strömgren 1963) from the strength of their balmer jumps. More recent work (Olsen 1984) has shown that the c_1 index is sensitive to surface gravity for the G- and early K-type stars as well. The use of the v filter in constructing the c_1 index is intended to remove the effects of metallicity, at least to first order, in the c_1 vs $b-y$ plane. Metallicity

TABLE 5. u by observations.

object	V	b-y	v-b	u-v	y_{err}	b_{err}	v_{err}	u_{err}
13.0-210	10.19	-0.01	0.35	0.82	0.02	0.02	0.00	0.00
13.0-228	11.75	0.37	0.50	0.98	0.00	0.00	0.00	0.00
13.0-256	17.83	0.26	0.57	0.77	0.00	0.01	0.00	0.16
13.0-301	16.74	0.42	0.46	0.75	0.00	0.00	0.00	0.13
9.0-185	15.21	0.43	0.59	1.12	0.00	0.00	0.00	0.01
9.0-187	13.73	0.36	0.46	0.93	0.00	0.00	0.00	0.00
9.0-197	15.05	0.59	0.88	1.30	0.00	0.00	0.00	0.07
9.0-169	15.76	0.44	0.61	1.11	0.00	0.00	0.01	0.03
9.0-194	13.23	0.37	0.35	0.89	0.00	0.00	0.00	0.01
9.0-188	15.66	0.51	0.63	1.06	0.00	0.00	0.01	0.01
9.0-179	14.63	0.48	0.49	1.04	0.00	0.00	0.00	0.01
9.0-483	17.46	1.00	0.16	1.27	0.02	0.21	0.17	0.07
9.0-186	13.58	0.33	0.46	0.93	0.00	0.00	0.00	0.01
9.0-195	16.67	0.33	0.44	0.79	0.00	0.00	0.00	0.05
9.0-170	16.67	0.37	0.56	0.87	0.00	0.01	0.01	0.02
9.0-172	16.89	0.27	0.62	1.42	0.01	0.02	0.01	0.10
9.0-183	12.78	0.42	0.61	1.07	0.00	0.00	0.00	0.01
9.0-167	16.70	0.63	0.94	1.86	0.00	0.00	0.03	0.05
9.0-171	17.64	0.42	0.56	0.87	0.00	0.00	0.07	0.14
9.0-192	16.47	0.35	0.42	0.82	0.00	0.00	0.03	0.04
9.0-572	16.83	0.41	0.54	1.08	0.00	0.00	0.07	0.03
9.0-107	14.59	0.35	0.44	0.85	0.00	0.00	0.00	0.01
9.0-122	15.08	0.39	0.51	0.90	0.00	0.00	0.00	0.02
9.0-132	15.07	0.43	0.62	1.06	0.00	0.00	0.00	0.03
9.0-111	16.78	0.43	0.69	1.26	0.00	0.00	0.01	0.04
9.0-112	17.47	0.42	0.40	0.89	0.00	0.01	0.01	0.01
2.0-094	16.55	0.55	0.72	1.14	0.00	0.00	0.00	0.03
2.0-139	16.78	0.43	0.64	0.90	0.00	0.00	0.00	0.03
2.0-095	11.42	0.39	0.57	0.91	0.00	0.01	0.01	0.00
2.0-075	13.67	0.54	0.68	1.15	0.00	0.00	0.00	0.02
2.0-096	14.55	0.89	1.18	1.57	0.00	0.00	0.00	0.09
2.0-029	16.89	0.59	0.66	1.10	0.00	0.00	0.00	0.03

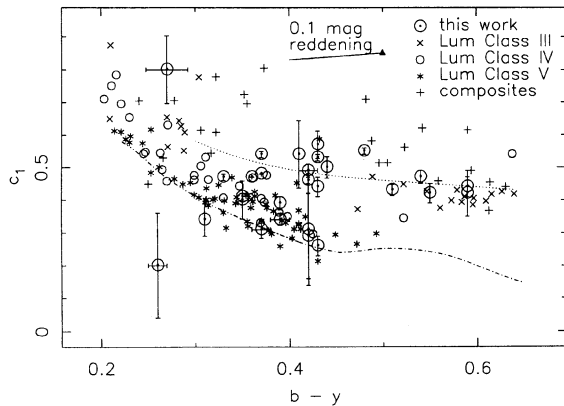


FIG. 6. The c_1 vs $b-y$ diagram for the 32 *uvby* observations, along with the POC standards of luminosity classes III, IV, V, and composites. The empirical population lines for luminosity class III (dotted line) and V (dot-dash line), along with the reddening vector, are also presented.

does affect the c_1 index, however, especially for the cooler giants. Figure 6 also presents the POC standards of luminosity classes III, IV, V, and composites, along with empirically-derived population lines. The dotted line above most of the stars is a fit to the luminosity class III stars of Ardeberg & Lindgren (1985). The lower dot-dash line is the standard relation for the Hyades dwarfs from Crawford (1975) for the bluer stars and Olsen (1984) for the redder stars. It can be seen that these lines follow the POC stars well. The reddening vector in this plane is also presented. The POC stars themselves are not corrected for reddening, since they are all very bright and thus relatively nearby.

Comparing the program objects which fall near the lower empirical relation to the POC data indicates that many of the program stars are dwarfs, while a few may be subgiants. The redder program objects match the POC luminosity class III giants. The two bluest objects plotted have the highest photometric errors, and seem somewhat unusual compared to the POC objects, though there are plenty of objects which lie in their respective portions of the c_1 - $b-y$ plane (e.g., supergiants, peculiar stars, red horizontal branch stars). The one red giant not plotted at $b-y=0.89$ lies very close to the luminosity class III empirical line. Such a comparison with the POC data, along with similar comparisons with metal-weak and peculiar

stars, as well as stars from open and globular clusters (presented in von Hippel 1991) constrain the luminosity classes for the bulk of the objects, and indicate that 90%–100% of all objects with $0.3 \leq b-y \leq 0.4$ are stars on, or just evolving off, the main sequence. Additionally, all objects with $b-y \geq 0.5$ are giants. These two color windows with constrained stellar luminosity classes, along with metallicity information provided by the survey, yield reliable absolute magnitudes for a limited subset of the survey population, the analysis of which is taken up in greater detail in Paper II.

4. CONCLUSIONS

In order to develop samples which best probe the thick disk population we have conducted a relatively deep three-color Strömgren photometric survey covering ≈ 1 square degree and including 1238 objects from 12 fields at various galactic locations. The data were acquired without kinematic or metallicity biases and are complete to $V=17.3$ – 18.5 , depending on the field, for 810 early to relatively late type (K0 V or G5 III) stars. Photometric metallicities were derived for 508 stars and indicate a metal-poor stellar population, consistent with a mixture of thick disk and halo stars.

Follow-up Strömgren *u*-band photometry was presented for 32 objects from the survey. The *u*-band photometry was used to study the population breakdown among the survey stars and indicates that stars at intermediate color ($0.3 \leq b-y \leq 0.4$) are predominantly main-sequence or slightly evolved stars, while redder survey stars ($b-y \geq 0.5$) are giants. The survey catalog is available in electronic form upon request.

This paper grew out of my thesis and I am deeply indebted to my advisor, Greg Bothun, for his many philosophical and scientific contributions. It is also a pleasure to thank Richard Sears, Doug Richstone, and Greg Aldering for their significant contributions; Gary Bower, Diab Jerrius, Stacy McGaugh, Chris Mihos, Jim Schombert, and Dave Silva for many useful discussions; Bob Barr, Larry Breuer, Peter Mack, and Matt Johns at MDM for assistance with the telescopes and instrumentation; Ed Carder and KPNO for the frequent use of their filters; the Michigan TAC for over sixty nights of telescope time; and the H. H. Rackham School of Graduate Studies for the Partnership in Research Grant, which supported much of this work.

REFERENCES

- Aldering, G. S., & Bothun, G. D. 1991, *PASP*, 103, 1296
 Ardeberg, A., & Lindgren, H. 1985, *IAU Symposium No. 111*, 509
 Bahcall, J. N. 1986, *ARA&A*, 24, 577
 Bahcall, J. N., & Soneira, R. M. 1980, *ApJS*, 44, 73
 Bahcall, J. N., & Soneira, R. M. 1984, *ApJS*, 55, 67
 Bergeron, P. 1989, private communication
 Bergeron, P., Wesemael, F., Fontaine, G., & Liebert, J. 1990, *ApJ*, 351, L21
 Burstein, D., & Heiles, C. 1982, *AJ*, 87, 1165
 Carney, B. W., Latham, D. W., & Laird, J. B. 1989, *AJ*, 97, 423
 Crawford, D. L. 1975, *AJ*, 80, 955
 Freeman, K. C. 1987, *ARA&A*, 25, 603
 Gilmore, G., & Reid, N. 1983, *MNRAS*, 202, 1025
 Graham, J. A. 1972, *AJ*, 77, 144
 Groth, E. J. 1986, *AJ*, 91, 1244
 Harris, W. E., Fitzgerald, M. P., & Reed, B. C. 1981, *PASP*, 93, 507
 Hintzen, P., Oswalt, T. D., Liebert, J., & Sion, E. M. 1989, *ApJ*, 346, 454
 Liebert, J., Dahn, C. C., & Monet, D. G. 1988, *ApJ*, 332, 891
 McCook, G. P., & Sion, E. M. 1987, *ApJS*, 65, 603
 Norris, J. 1986, *ApJS*, 61, 667

- Norris, J. 1987, ApJ, 314, L39
Norris, J., Bessell, M. S., & Pickles, A. J. 1985, ApJS, 58, 463
Norris, J. E., & Green, E. M. 1989, ApJ, 337, 272
Norris, J. E., & Ryan, S. G. 1989, ApJ, 340, 739
Olsen, E. H. 1984, A&AS, 57, 443
Perry, C. L., Olsen, E. H., & Crawford, D. L. 1987, PASP, 99, 1184 (POC)
Sandage, A. 1987, AJ, 93, 610
Sandage, A., & Fouts, G. 1987, AJ, 93, 74
Schuster, W. J., & Nissen, P. E. 1989, A&A, 221, 65 (SNII)
Strömgren, B. 1963, in Stars and Stellar Systems, edited by K. Aa. Strand (University of Chicago Press, Chicago), Vol. 3, p. 123
von Hippel, T. A. 1991, Ph.D. thesis, University of Michigan
von Hippel, T. A., & Bothun, G. D. 1992, ApJ (submitted) (Paper II)
Winget, D. E. *et al.* 1987, ApJ, 315, L77
Wyse, R. F. G. & Gilmore, G. 1986, AJ, 91, 855
Wyse, R. F. G., & Gilmore, G. 1988, AJ, 95, 1404